

Algorithm-Based Optimization of Gear Mesh Efficiency in Stepped Planetary Gear Stages for Electric Vehicles

Christian Westphal, Jens Brimmers and Christian Brecher

Introduction and Motivation

Increasing demands on product performance have led to high demand for optimization in component design. Optimization methods can be used to solve the conflicts between different design objectives. The importance of numerical optimization methods is also increasing in the gear design and is part of different phases of the development process. The gear design is divided into four essential steps, which are necessary for the definition of the macro- and microgeometry of the gears (Ref. 1).

The process shown in Figure 1 starts with the determination of the gearbox topology. The topology is largely derived from the gear ratio requirement between driving and driven components. Methods for optimizing the transmission topology are based on simplified standard calculations and evaluating various transmission topologies. The possible topologies are evaluated concerning their volume, the expected efficiency, and the achievable load-carrying capacity. At this early stage of development, these parameters can only be determined approximately since the macrogeometry of the gears and the shaft bearing system have not been defined yet. With the gear topology selected, the gears can be designed, see Figure 1. The boundary conditions for designing the gear stages, such as the center distance, the gear ratio, and the face width, have been defined in the previous step. A design of gears with a focus on the load-carrying capacity is possible according to ISO 6336 (Ref. 2). If other design objectives are in focus, such as efficiency

or excitation behavior, higher-level methods are recommended. With a variant calculation, the selection of a gear geometry corresponding to the requirements is possible. With an increasing number of variation variables, numerical optimization methods can be more target-oriented compared to variant calculations. For the final evaluation of the operational behavior, for example, FE-based methods can be used (Refs. 3 and 4).

In the third step of the gearbox design, further components such as shafts, bearings and the housing are designed, see Figure 1. The transmitted forces and torques are completely defined at this development step. Especially for gearboxes with a high required power density, an iterative procedure within the first three design steps may be necessary (Ref. 1). The last and fourth step of the gear design is the optimization of the tooth contact with a specifically designed microgeometry. The level of detail of the design is the highest in this step, so numerical methods are often used. When designing the microgeometry, manufacturing deviations and load-dependent misalignments can be considered. FE-based variant calculations are suitable for determining an optimal microgeometry. Further optimization potential in this design step is provided, for example, by topological flank modifications (Refs. 5 and 6).

Optimization methods can be usefully applied in every step of the gear design process. Especially for gearboxes with more complex kinematic relationships and additional geometric restrictions that vary depending on the design parameters, as it

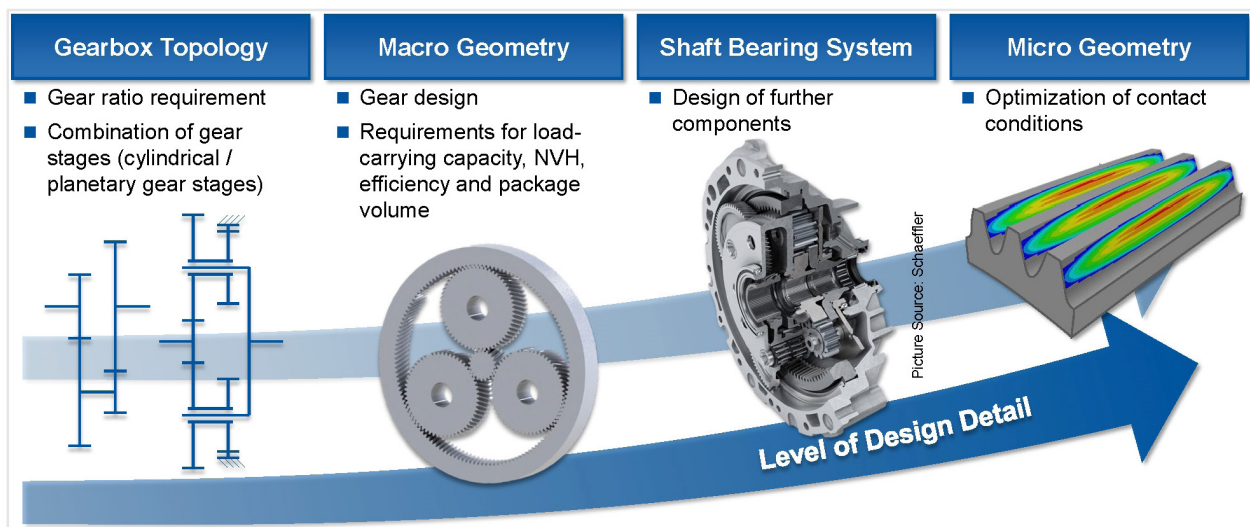


Figure 1 Gearbox Design Process

Printed with permission of the copyright holder, the American Gear Manufacturers Association, 1001 N. Fairfax Street, 5th Floor, Alexandria, Virginia 22314. Statements presented in this paper are those of the authors and may not represent the position or opinion of the American Gear Manufacturers Association.

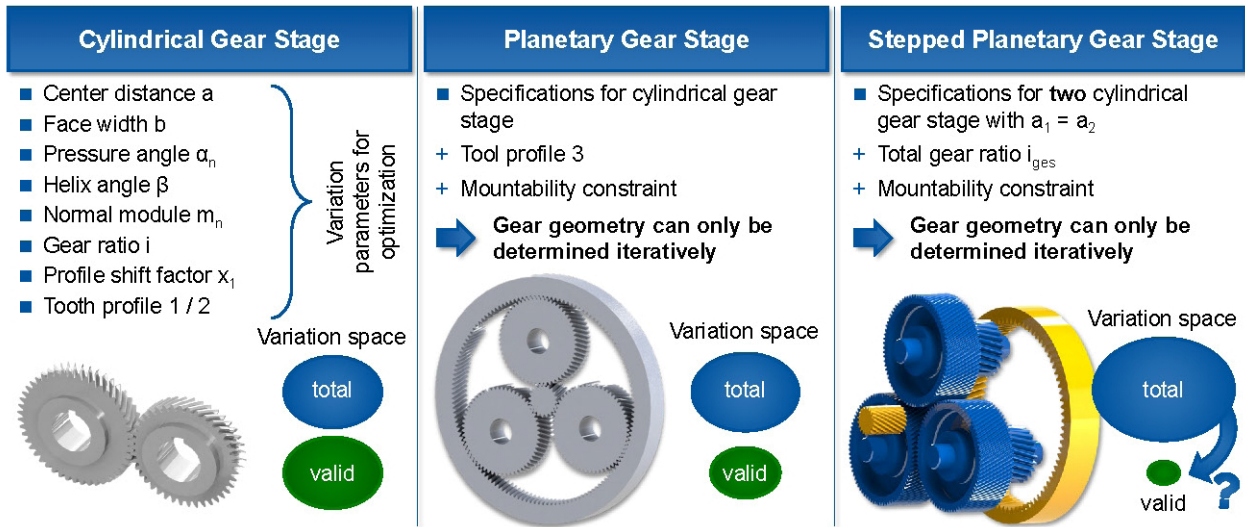


Figure 2 Variation Parameters and Constraints in the Design of Stepped Planetary Gear Stages

is with the case of planetary gear stages, numerical optimization methods can make further potential available.

Design of Stepped Planetary Gear Stages

One of the challenges in the design of automotive transmissions is the combination of high power density, high efficiency, and low noise excitation. With the electrification of the powertrain, the requirements in terms of noise excitation and efficiency increase further. On the one hand, the masking noise of the combustion engine is eliminated, and on the other hand, energy efficiency is mandatory for electric vehicles. To meet these requirements, complex transmission topologies with planetary gear stages are increasingly being used. Advantages of planetary gear stages are, in particular, the short axial length in conjunction with the coaxial alignment of the input and output shafts and the comparatively high gear ratio and power density. To increase the power density and the maximum achievable gear ratio further, stepped planetary gear stages (also called compound epicyclic) can be used. In these, a stepped planet consisting of two rigidly connected gears is used instead of one single planet. The input shaft of the stepped planetary gear stage considered in the following is the sun. The ring gear is fixed to the housing and the output shaft is the planet carrier.

With this gear configuration, ratios between sun and carrier of $i_{SC} \geq 20$ are possible, considering geometric boundary conditions. The stationary gear ratio i_0 is calculated according to Equation 1, which describes the gear ratio with a planet carrier fixed to the housing, input on the sun and output on the ring gear. The stationary gear ratio i_0 is used to derive the gear ratio i_{SC} of the relevant configuration with the ring gear fixed to the housing, input on the sun, and output on the planet carrier, according to Equation 2 (Ref. 7).

$$i_0 = - \frac{z_{P1} \cdot z_R}{z_S \cdot z_{P2}} \quad (1)$$

$$i_{SC} = 1 - i_0 = 1 + \frac{z_{P1} \cdot z_R}{z_S \cdot z_{P2}} \quad (2)$$

where

i_0 is the stationary gear ratio [-]

i_{SC} is the gear ratio between the sun gear and carrier [-]

z_S is the number of teeth of the sun gear [-]

z_{P1} is the number of teeth of the first planet [-]

z_{P2} is the number of teeth of the second planet [-]

z_R is the number of teeth of the ring gear [-]

The description of the macrogeometry of cylindrical gear stages requires the specification of certain parameters, which define the geometry without contradiction. Based on these parameters, further macrogeometry parameters can be calculated. Some of the most important values for the geometry calculation of cylindrical gear stages are shown in Figure 2 on the left. For example, the sum of the numbers of teeth Σ_z can be calculated from the center distance a , the helix angle β and the normal module m_n , assuming backlash-free gears without profile shift (Ref. 2). The sum of the numbers of teeth Σ_z is then divided between the two gears, taking the gear ratio i into account. The tip diameter of the first gear is calculated from the tooth root shape of the counter gear and the required tip clearance. In the case of sharp teeth, the tip circle diameter must be reduced so that a minimum tooth thickness is achieved at the tip circle diameter. If the geometry parameters are varied within reasonable limits, the result is a variation space with just geometrically valid gears. The limits of the variation space are not identical for every application. For example, the module m_n should only be increased until the undercut limit is reached on the pinion. Between the minima and maxima, the variation

variables lead to valid geometries.

In the design of planetary gear stages, it is necessary to consider characteristics concerning the kinematic couplings. The kinematics of a planetary gear stage is completely determined by one planetary gear. With each additional planetary gear, a kinematic overdetermination takes place, which results in the fact that only special tooth number combinations enable uniform distribution of the planetary gears in the carrier. For simple planetary gear stages, the number of teeth of the sun and the ring gear must fulfill Equation 3. This assembly condition is transferable to stepped planetary gear stages. For a uniform distribution of the planet gears in the carrier, Equation 4 must be fulfilled for stepped planetary gear stages (Ref. 7).

If a variant calculation is carried out for planetary gear stages, an additional variation variable is required for the tool profile of the ring gear, see Figure 2 center. For simple planetary gear stages, due to the double gear mesh on the planetary gear, most of the macrogeometry parameters in both meshes are identical or can be calculated directly. Due to the assembly condition, this calculation also results in nonvalid tooth number combinations, so an iterative calculation is necessary and only a subset of the variation space can be considered further. An additional limitation of the variation space can be made, for example, by the exclusive selection of variants with numbers of teeth without a common divisor.

$$|z_S| + |z_R| = n_p \cdot j \tag{3}$$

$$|z_S \cdot z_{p2}| + |z_{p1} \cdot z_R| = n_p \cdot j \tag{4}$$

where

- z_S is the number of teeth of the sun gear [-]
- z_R is the number of teeth of the ring gear [-]
- z_{p1} is the number of teeth of the first planet [-]
- z_{p2} is the number of teeth of the second planet [-]
- n_p is the number of (stepped) planets [-]
- j is an integer [-]

In the case of stepped planetary gear stages, two geometrically independent gear meshes can be designed and optimized, see Figure 2 on the right. The number of variation variables and thus the number of theoretically available geometry variants is,

accordingly, significantly higher. At the same time, the assembly condition according to Equation 4 must be observed, which limits the valid variation space. The numbers of teeth resulting from the gear ratios of the sub-stages must also satisfy the required total gear ratio i_{SC} between sun and carrier, according to Equation 2. Overall, this results in a comparatively large variation space that contains only a few valid geometries. Due to the described restrictions, which can be extended by the exclusive selection of variants with numbers of teeth without a common divisor, an iterative geometry calculation for stepped planetary gears is necessary.

If a comprehensive variation of the parameters of the macrogeometry as well as of the tool profile is performed for all gears, many possible combinations arise. Algorithm-based optimization methods are suitable for selecting a variant within such a large variation space. A full factorial calculation of all geometry variants with high-level calculation methods is not possible in a reasonable calculation time. Nevertheless, with the independent design of the two sub-stages, an increase in power density and efficiency through optimized geometry parameters is conceivable. In the literature, no numerical optimization of the gear geometry of stepped planetary gears is known that combines a tool-based geometry calculation with an FE-based tooth contact analysis.

Objective and Approach

Stepped planetary gear stages can be used to increase the power density in electrically driven vehicles. However, assembly constraints must be considered during design and optimization, which, in combination with a large number of variation variables, require algorithm-based optimization methods. In the design of gearboxes, various design objectives are relevant, which cause conflicts. Therefore, the objective of this paper is the development of a method for algorithm-based design and optimization of the macrogeometry of stepped planetary gear stages, considering weighted design objectives, see Figure 3.

To achieve the overall objective, the boundary conditions in the design of stepped planetary gear stages are first analyzed

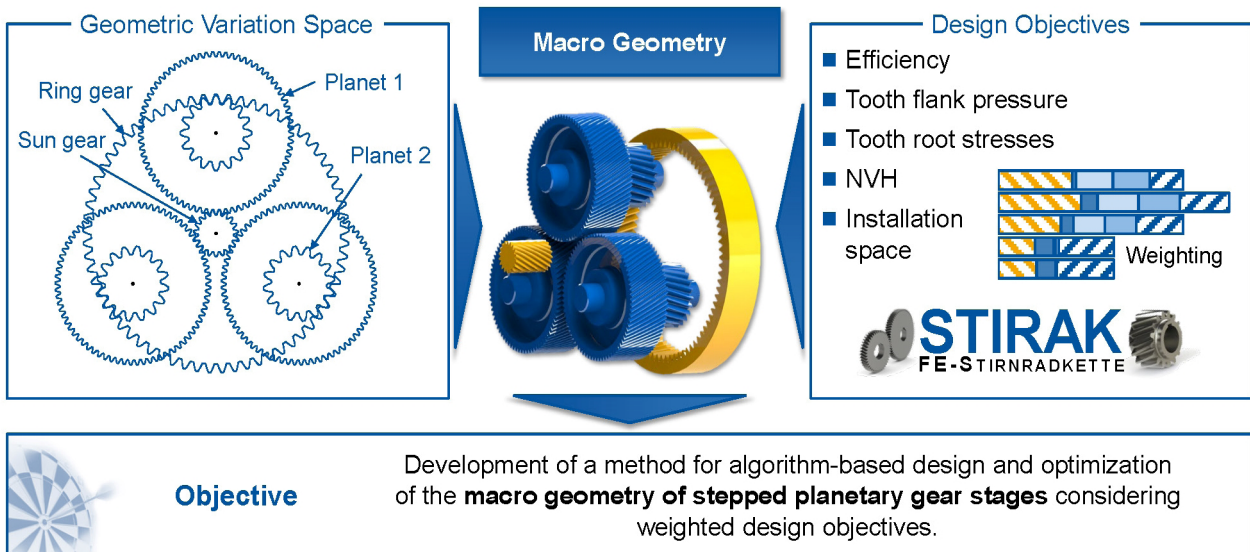


Figure 3 Objective and Approach

in more detail and the geometric variation space is defined. The angular positions of the stepped planets for assembly are derived considering the phase position of the gear meshes. Subsequently, an optimization algorithm is selected that allows an application-oriented evaluation of the gear geometry. The design objectives efficiency, load-carrying capacity, NVH (Noise, Vibration, Harshness), and volume are weighted for different operating points. The operational behavior of the gear geometries is evaluated using the FE-based tooth contact analysis FE-STIRNRADKETTE (Ref. 3). The developed method is then applied to a stepped planetary gear stage of an electrically driven compact car. Different weighting variants of the design objectives are investigated, and the results are compared.

Boundary Conditions for the Design of Stepped Planetary Gear Stages

The assembly constraint of stepped planetary gear stages results from the kinematic coupling of the gear meshes and consequent geometrical restrictions. In this chapter, a method is first presented that enables the identification of suitable tooth number combinations. Subsequently, the phase position of the gear meshes and the necessary assembly angles of the stepped planets are derived. It is assumed that the angle between planet 1 and planet 2 of the same shaft is identical for each of the mounted stepped planets and that they are therefore interchangeable.

Identification of Suitable Numbers of Teeth Combinations

In contrast to simple cylindrical gear stages, the calculation of the numbers of teeth of stepped planetary gear stages is constrained by the mountability. The equation for verifying the mountability was explained in “Design of Stepped Planetary Gear Stages,” see Equation 4. Due to the high number of non-mountable geometry variants, a variation of the numbers of teeth with an optimization algorithm is not effective. The number of iterations required to achieve convergence in the optimization can be reduced by avoiding the calculation of non-mountable geometry variants. To exclude these variants, a method for identifying suitable numbers of teeth is presented in the following section. This method uses eight input parameters

that lead to one optimal numbers of teeth combination. The eight input parameters can be varied by the optimization algorithm so that only mountable geometry variants are compared during optimization.

The entire procedure for determining the numbers of teeth is shown in Figure 4. The numbers of teeth of the stepped planetary gear stage are determined depending on the eight parameters shown in Figure 4 at the bottom. First, the possible numbers of teeth of the four gears (sun gear, planet 1, planet 2, and ring gear) are varied full factorially in defined ranges. With these, the total gear ratio i_{SC} is calculated in step 2 according to Equation 2. Only variants with a maximum deviation of the total gear ratio of $\Delta i = 0.4$ are selected for further consideration. The number of remaining variants has decreased significantly with this step, see Figure 4.

In the third step, the gear ratio of the first stage (sun-planet 1) of all variants is compared with the target gear ratio of the first stage and used to reduce the number of remaining variants. The permissible deviation of the gear ratio of the first stage is evaluated less restrictively than that of the overall gear ratio since the gear ratio of the first stage is taken up again in step 6. An additional constraint in the identification of the numbers of teeth is the limitation of the greatest common divisor of adjacent gears to $\text{gcd}(z_1; z_2) = 1$, see step 4 in Figure 4. For the remaining variants, the mountability is checked in step 5 according to Equation 4. In addition, a penetration check of the tip diameters of the planet gears is performed, considering the number of stepped planets n_p . The resulting variants contain all tooth number combinations that fulfill the gear ratio requirements and are mountable. In the sixth step, the stepped planetary gear stage is scaled with the center distance a to calculate the normal module m_n of the stages. In the calculation, it is first assumed that the gears are designed without profile shifts and that the center distance a corresponds to the zero center distance $ad = a$. According to Equation 5, the resulting normal module of each variant $m_{n,var}$ is calculated for both stages. Finally, the variant with a minimum combined deviation according to Equation 6 is selected, see Figure 4, step 6. The deviations from the target values of the normal module of stage 1 $m_{n,1}$, the normal module $m_{n,2}$ of stage

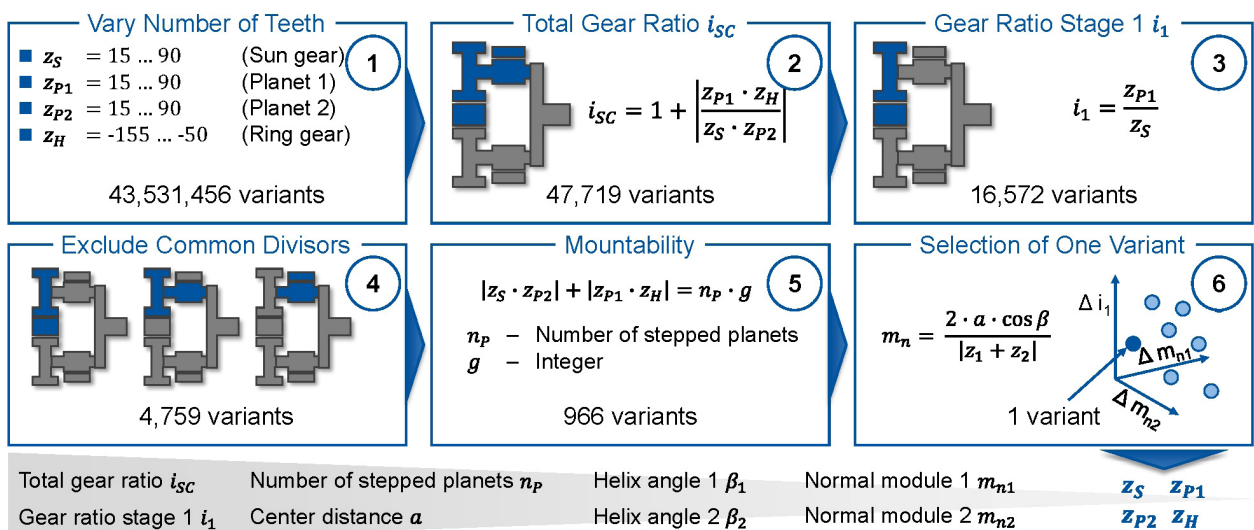


Figure 4 Iterative Identification of Suitable Numbers of Teeth Combinations

2 and the gear ratio of stage 1 i_1 are weighted equally.

$$m_{n,var} = \frac{2 \cdot a_d \cdot \cos \beta}{\sum z} \quad (5)$$

$$\min \left(\sqrt{m_{n,1} - \frac{2 \cdot a_d \cdot \cos \beta_1}{z_S \cdot z_{P1}}}^2 + \left(m_{n,1} - \frac{2 \cdot a_d \cdot \cos \beta_2}{z_{P1} \cdot z_H} \right)^2 + \left(i_1 - \frac{z_{P1}}{z_S} \right)^2 \right) \quad (6)$$

where

z is the number of teeth [-]

a_d is the zero center distance [mm]

β is the helix angle [°]

m_n is the normal module [mm]

Phase and Assembly Position

Since the mountability of the stepped planetary gear stage is ensured with a suitable numbers of teeth combination, this section considers the necessary positioning of the stepped planets for assembly. As described at the beginning of this chapter, the angle between the two planet gears is assumed to be identical for all stepped planets. In addition, the stepped planets are to be evenly distributed around the circumference of the planet carrier.

A sketch of the gear teeth in assembly position is shown in Figure 5, left. As shown in detail view A, the first tooth gap of the ring gear is in the upper position and is marked with the number 1. The numbering of the tooth gaps on the central gears and the teeth on the planets is in the mathematical positive direction around the z -axis — counterclockwise. The first tooth gap of the sun gear is aligned in the direction of the y -axis. Planet 1 of stepped planet 1 in the sun contact is accordingly aligned with tooth 1 downward in the negative y -direction, see detail view B in Figure 5, right. Planet 2 of stepped planet 1 is oriented upward with tooth 1 in the y -axis direction. With this definition, the positions of the central gears and the stepped planet 1 are fixed. To visualize the rotation angles of the stepped planets, tooth 1 of planet 1 and tooth 1 of planet 2 of each stepped planet are marked with points and are connected with a line.

The calculation of the assembly angle of the second and third stepped planets is derived based on the phase position of the gear meshes of the planet gears and the central gears. First, the phase position of the meshes with the central gears is calculated.

The calculation for the sun-planet 1 meshes Δp_{Si} is done according to Equation 7 and correspondingly for the planet 2-ring gear meshes Δp_{Hi} according to Equation 8. The angle $\varphi_{Pin,i}$ describes the angle between the vertical (y -axis) and the connecting line between the centers of the sun and the stepped planet i in the mathematical positive direction. The phase shift in the sun mesh is then converted into a rotation angle of planet 1, see Equation 9. This rotation angle $\varphi_{Pi,\Delta pS}$ ensures that planet 1 is correctly aligned in the sun mesh right, see Figure 5. In the further procedure, the stepped planet i consisting of planet 1 and planet 2 is iteratively rotated by one pitch in the sun-planet 1 mesh, until the phase shift in the planet 2-ring gear mesh corresponds to the previously calculated value Δp_{Hi} . The calculation of the phase shift in the planet 2-ring gear mesh from the rotation of the stepped planet is described in Equation 10. The integer j corresponds to the number of pitches necessary to obtain the required phase shift in the planet 2-ring gear mesh. Finally, the rotation angle for the assembly of the stepped planet i is calculated from the sum of the two angles $\varphi_{Pi,\Delta pS}$ and $\varphi_{Pi,\Delta pR}$, see Equation 11.

$$\Delta p_{Si} = \text{mod} \left(\varphi_{Pin,i} \cdot \frac{z_S}{2 \cdot \pi}, 1 \right) \quad (7)$$

$$\Delta p_{Ri} = \text{mod} \left(\varphi_{Pin,i} \cdot \frac{|z_R|}{2 \cdot \pi}, 1 \right) \quad (8)$$

$$\varphi_{Pi,\Delta pS} = \Delta p_{Si} \cdot \frac{2 \cdot \pi}{z_{P1}} \quad (9)$$

$$\Delta p_{Ri} = 1 - \text{mod} \left(\frac{\varphi_{Pi,\Delta pS} + j \cdot \frac{2 \cdot \pi}{z_{P1}}}{\frac{2 \cdot \pi}{z_{P2}}}, 1 \right) \quad (10)$$

$$\varphi_{Pi} = \varphi_{Pi,\Delta pS} + \varphi_{Pi,\Delta pR} = \varphi_{Pi,\Delta pS} + j \cdot \frac{2 \cdot \pi}{z_{P1}} \quad (11)$$

where

Δp_{Si} is the phase position of the sun-planet 1 meshes [pet]

Δp_{Ri} is the phase position of the planet 2-ring gear meshes [pet]

$\varphi_{Pin,i}$ is the angle of the planet pin position in the carrier [rad]

$\varphi_{Pi,\Delta pS}$ is the rotation angle of the stepped planet due to the phase position in the sun gear mesh [rad]

$\varphi_{Pi,\Delta pR}$ is the rotation angle of the stepped planet due to the phase position in the ring gear mesh [rad]

$z_{S/P1/P2/R}$ is the number of teeth of the sun / planet 1 / planet 2 /

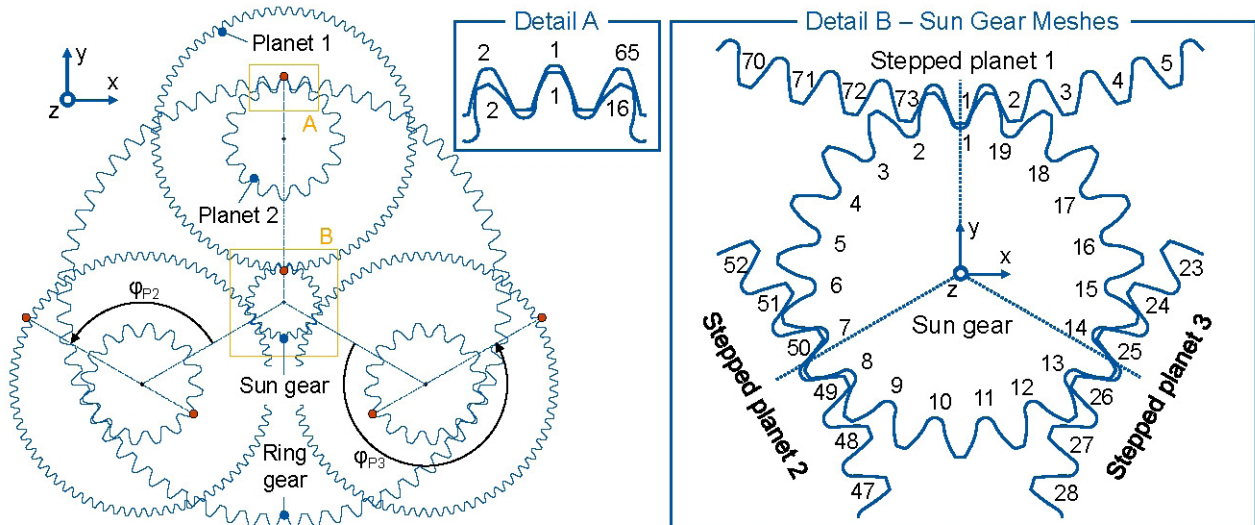


Figure 5 Sketch of the Stepped Planetary Gear Stage in Assembly Position

ring gear [-]
 j is an integer [-]
 φ_{Pi} is the rotation angle for the assembly of the stepped planet I [rad]

FE-based Macrogeometry Optimization

Numerical optimization methods are used in various engineering areas. In the gearbox design, for example, topology optimization of the housing can be used to reduce the housing mass and increase the stiffness. Optimization of the macro- and microgeometry of the gears is increasingly in focus.

In this paper, a particle-swarm algorithm is used, which is described in more detail in the following section. Then, the constraints, optimization variables, optimization objectives, and their weighting are presented. In contrast to existing optimization methods, an FE-based tooth contact analysis is used to evaluate the operational behavior. Furthermore, a comprehensive variation of different geometry parameters is performed.

Set-up of the Optimization Method

When optimizing the macrogeometry of stepped planetary gear stages, various boundary conditions must be considered. First, a total gear ratio i_{total} is assumed for the specific application. The number of stepped planets and the microgeometry of the gears are specified as further constraints. For the microgeometry, only a lead crowning and a profile crowning are used. The operating points and evaluation criteria as the last constraints are explained in the next section.

The optimization procedure, the boundary conditions and the optimization parameters are shown in Figure 6. The developed optimization method is based on a particle swarm algorithm with 60 individuals per generation. As can be seen on the right side of Figure 6, the method consists of two processes. First, the particle swarm algorithm creates the input parameters of the next generation. These are computed and evaluated one after the other before the results are provided to the algorithm again and it derives a set of optimized input parameters for the next generation. The total number of generations calculated was chosen as the termination criterion.

When calculating the geometry of the individual variants, the

procedure for identifying suitable numbers of teeth is applied as described in the sections before. The geometry parameters that are varied and optimized are listed in Figure 6, bottom left. Since the calculation of the numbers of teeth assumes that the gear teeth are designed without profile shift, the parameter *module deviation* Δm_n is introduced for each gear mesh. With this, the optimization algorithm allows a specific change to the normal module resulting from the calculation of the numbers of teeth. With this change, a sum profile shift becomes necessary at the same time, which is divided between the two gears belonging to one gear mesh with the optimization parameter *profile shift distribution* x_1/x_2 . The tool profile for the geometry calculation of the gear teeth is fully rounded at the tip for all calculations. The addendum factor of the tool profile h_{ap0}^* is optimized and thus the tooth root shape is also integrated into the optimization. In total, 18 optimization parameters result, which define the variation space.

The calculation of the characteristic values of each variant is performed with the FE-based tooth contact analysis FE-STIRNRADKETTE. The single gear meshes are calculated independently of each other under quasistatic conditions. Since the shaft-bearing system has not been defined at that stage of design and therefore no load-dependent misalignments can be calculated yet, an ideal alignment of the gear teeth is assumed, see Figure 1. The characteristic values for evaluation and weighting are presented in the following section.

Optimization Objectives and Weighting

In the gear design, the five design objectives load-carrying capacity, excitation behavior, efficiency, cost, and volume can be identified (Ref. 1). With the method presented in this paper, a comprehensive evaluation of all objectives, except cost, is performed. The load-carrying capacity is considered differentiated in terms of maximum tooth flank pressure and maximum tooth root stress. The excitation behavior is evaluated with the peak-to-peak transmission error and the efficiency with the load-related power loss in the gear mesh. The volume is evaluated based on an enveloping cylinder.

The evaluation of the objective values is done with a linear

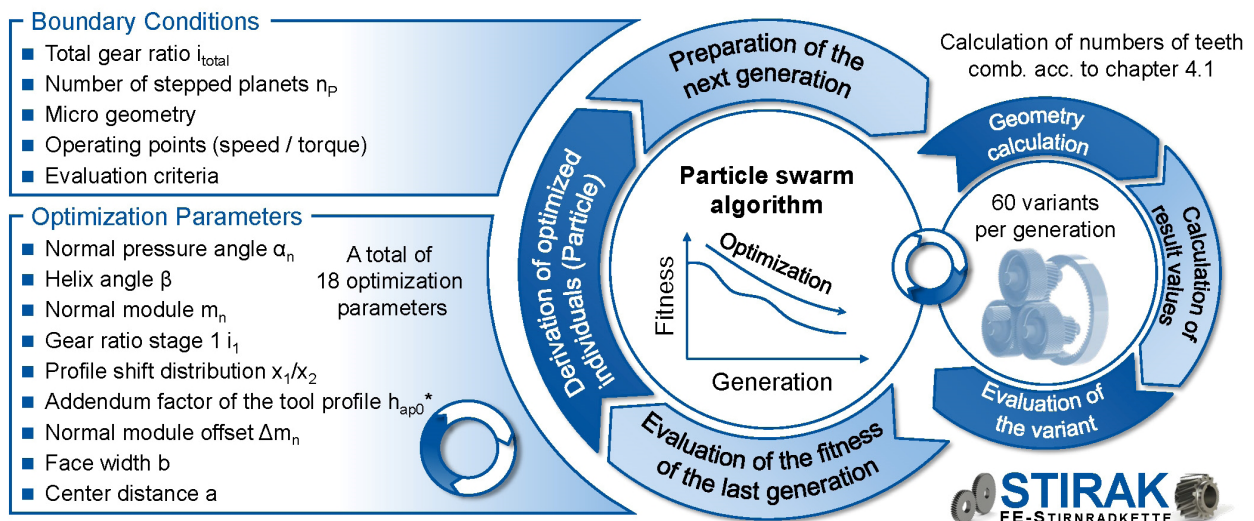


Figure 6 Procedure of the Optimization Method

grade scaling (1–best and 6–worst) for comparability among them. The calculation of the grade gr is shown in Equation 12 for a quantity to be minimized for different cases. If the calculated value v exceeds the limit value of the grade 6 v_6 , an additional deterioration of the grade is applied. This procedure prevents the compensation of different parameters in impermissible ranges.

$$gr = \begin{cases} 1 & v \leq v_1 \\ 1 + \frac{5}{v_6 - v_1} \cdot (v - v_1) & v_1 < v \leq v_6 \\ 6 + \left(\left(1 + \frac{5}{v_6 - v_1} \cdot (v - v_1) \right) - 6 \right) \cdot 5 & v_6 < v \end{cases} \quad (12)$$

where
 gr is the grade
 v is the value to be graded
 v_1 is the value related to grade 1 (best)
 v_6 is the value related to grade 6 (worst)

Various operating points consisting of speed and torque are relevant in the gear design. The weighting of the objective values can be different for each operating point. To evaluate a geometry variant, FE-based tooth contact analysis is used to perform calculations at different operating points. Subsequently, the parameters are individually evaluated with grades. The overall evaluation of the geometry variant is calculated according to Equation 13. The procedure for determining the weighting factors of the objective values $w_{k,OP}$ required for the overall evaluation is shown in Figure 7.

$$f = \sum_{op=1}^{n_{op}} \sum_{k=1}^{n_k} w_{k,OP} \cdot gr_{k,OP} \quad (13)$$

where
 f is the function value
 k is the identifier of the objective value
 n_k is the number of objective values
 OP is the identifier of the operating point
 n_{OP} is the number of operating points
 $w_{k,OP}$ is the weighting of the objective value k at the operating point OP
 $gr_{k,OP}$ is the grade of the objective value k at the operating point OP

Five relevant operating points were identified for the design, see Figure 7, bottom right. First, the weighting of the design

objectives is determined for each operating point, see step 1. The volume of the gear stage is equally relevant for each operating point. In this example, the excitation in the form of the peak-to-peak transmission error is of higher interest in lower torque ranges. In contrast, the characteristic values for the load-carrying capacity are weighted higher at higher torques. In addition to the weighting of the design objectives for each operating point, the weighting of the operating points among each other is also possible. In the example shown, the operating points with higher torque were weighted higher overall, see Figure 7, bottom left. The weighting factors are then normalized so that different weighting variants can be compared, see Figure 7, top right.

Application of the Optimization Method

In this chapter, the developed method for optimizing a stepped planetary gear stage is applied to an electrically driven compact car. First, the use case and the resulting boundary conditions for the optimization are presented. Then, the different weighting variants for the optimization are described and compared. Finally, the optimization results are analyzed and compared with the initial gear design.

Boundary Conditions of the Optimization

The application of the developed method is carried out using the example of an electrically driven compact car. A conventionally driven VW Golf 7 GTI with a maximum output of $P_{max} = 160$ kW was chosen as a reference for comparison. To identify the required boundary conditions of the gearbox, the wheel torque of the conventionally driven vehicle with a 6-speed transmission was plotted against the vehicle speed in Figure 8.

The torque-speed characteristics with six gears of the conventional drivetrain can be approximated with a torque-speed characteristic of an electrical machine. The total power required by the drive unit is divided between two electrical machines, which can be used, for example, as single-wheel drives. The maximum driving speed of the vehicle is limited to $v_{max} = 180$ km/h. With the maximum speed of the electrical machines $n_{EM,max} = 25,000$ rpm, the required gear ratio $i_{ges} = 16.60$ is calculated, see step 1 in

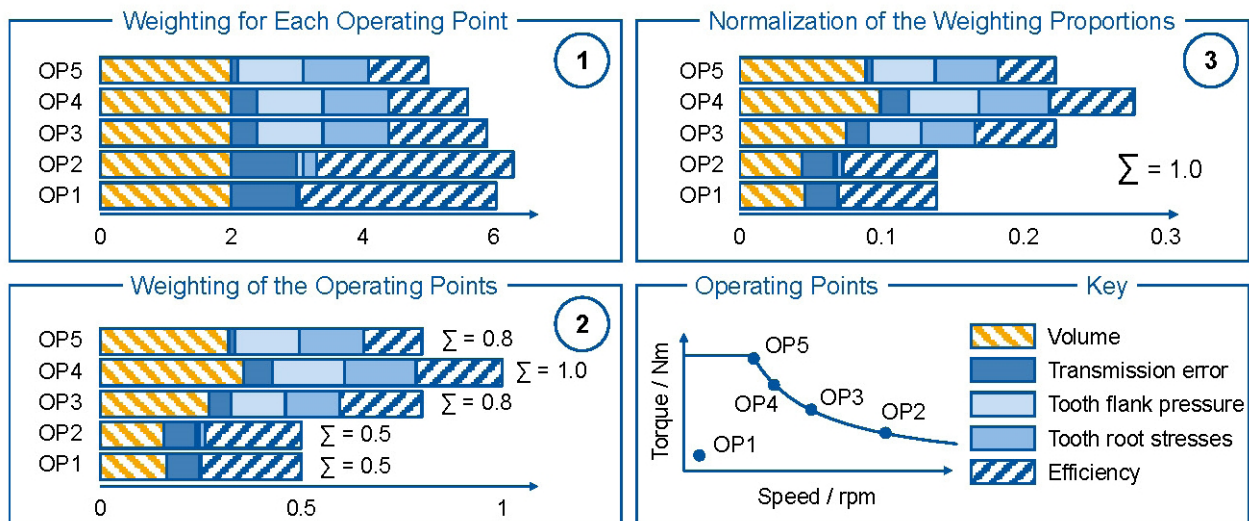


Figure 7 Determination of Weighting Factors for Different Operating Points

Figure 8. A stepped planetary gear stage is therefore suitable for achieving the required total gear ratio. The maximum achievable torque of the electrical machines is then derived from the rated speed of the electrical machine, see step 2 in Figure 8.

Five operating points are identified for the design of the gear stage. The first operating point, OP1, has a low torque and is used during optimization mainly to limit the excitation in the low torque range. The other four operating points are on the maximum power hyperbola and cover a wide torque and speed range.

Description of the Optimization Variants

Ten different weighting variants are selected to optimize the stepped planetary gear stage, see Figure 9. The weighting of the efficiency and the volume is set differently for the variants. The weighting of the remaining optimization objectives — i.e., peak-to-peak transmission error, tooth flank pressure, and tooth root stress — changes accordingly. Starting from variant V11 at the top left in Figure 9, the weighting of the efficiency increases with the variants to the right. The weighting of the volume is

increased downwards to variant V14.

A general overview of the variants can be seen in Figure 9, bottom right. The four highlighted weighting variants will be considered in more detail in the next section, as they represent the extrema of the different weightings. In total, three inter-related variant series can be identified. In the variant series V11-V21-V31 and V12-V22-V32-V42-V52, the share of efficiency weighting is progressively increased. The share of volume weighting is progressively increased for the variant series V11-V12-V13-V14. The weighting of the operating points among each other leads to a design focus on the higher torque operating points OP3 to OP5.

Analysis of the Optimization Results

The optimization process of the stepped planetary gear stage was stopped after 100 generations for each weighting variant. A total of 6,000 different geometries were calculated and compared for each weighting variant at five operating points each. For further analysis, the variants were recalculated with a finer resolution of the FE model of the gears. The resulting objective

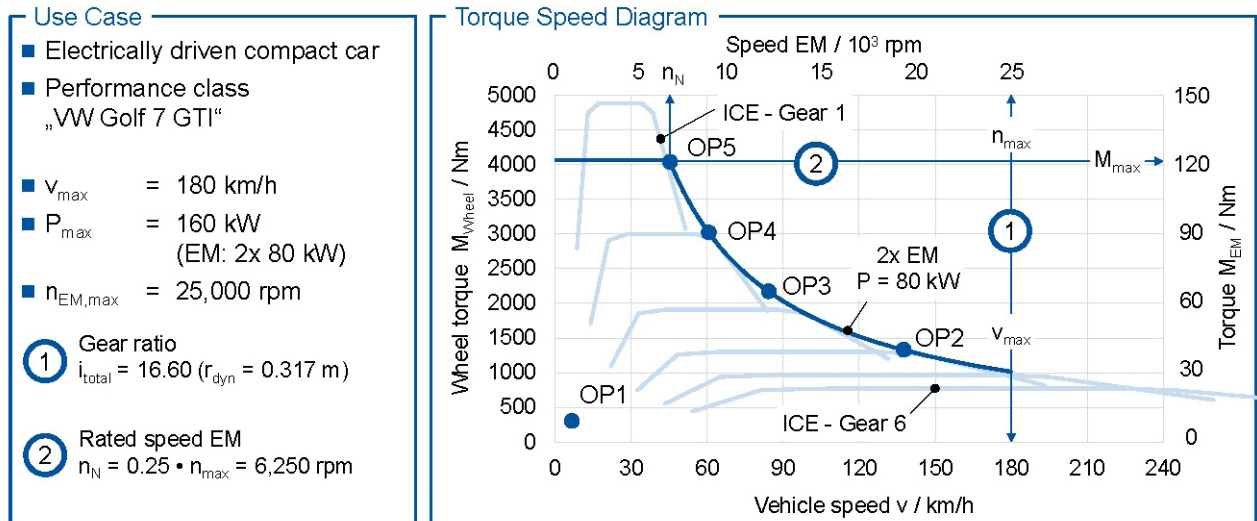


Figure 8 Torque Speed Diagram of the Electrical Machine (EM) and Derivation of Relevant Operating Points (OP)

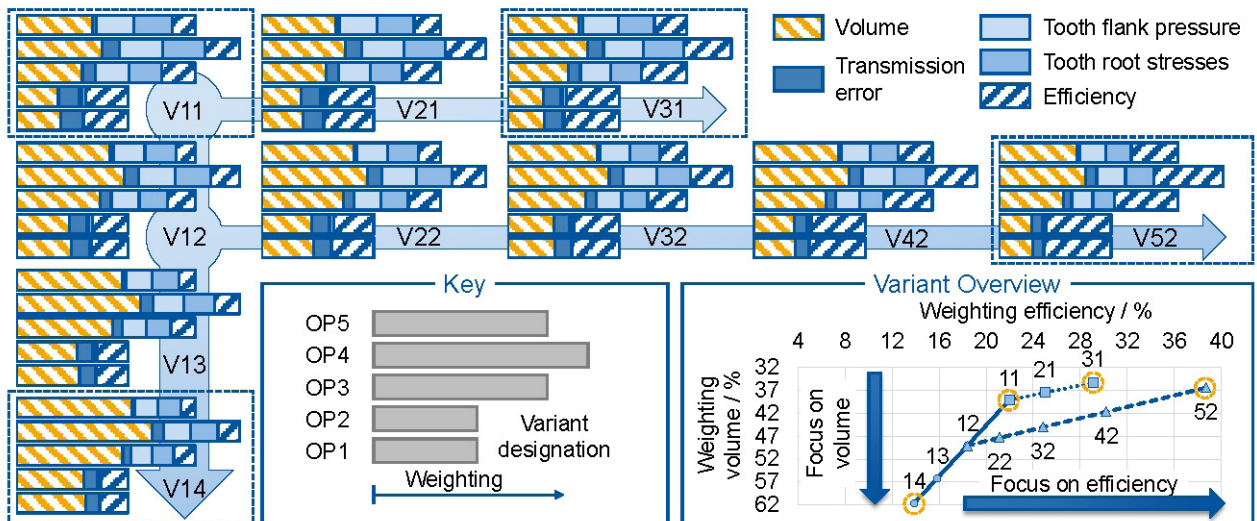


Figure 9 Weighting Variants

values of the optimizations are shown in Figure 10. The theoretical volume of the gear is calculated from the maximum outer diameter and the sum of the face width of the two gear meshes. In Figure 10, top left, the volume of the variants is plotted against the weighting share of the volume. The results show an approximately linear relationship between the weighting and the volume. Variant V14, with the highest weighting of the volume, achieved a 34.3% lower volume than variant V31. The correlations of the different weighting series are recognizable and verify the optimization method.

The results of the second optimization objective, efficiency, are shown in the top right of Figure 10. The diagram shows the mean value of the efficiencies of the two gear meshes for the highest weighted operating point OP4, above the weighting of the efficiency. The increase in the mean efficiency with increasing weighting is visible. The variants converge to a maximum as the weighting increases.

Due to the variation of the two optimization objectives volume and efficiency, the weighting of the other optimization objectives also changes. The results of the other objective values are shown in the same form in Figure 10 below. In particular,

the tooth flank pressure and the tooth root stress show a very good correlation between weighting and value.

Four weighting variants were selected for further analysis. The designation and a comparison of the volumes of the different variants can be found in Table 1. With these four variants, the extrema of the weighting series are covered and can be compared with the initial design start. The difference between the variants V31 and V52 is the weighting of the efficiency compared to the weighting of the other optimization objectives. The weighting of the volume is similar so that for variant V31 it can be concluded that the higher volume has a positive influence on the tooth flank pressure and the tooth root stress, see Figure 10 bottom.

Table 1 Theoretical volume of the selected variants			
Variant	Main optimization objective	Theoretical volume / l	Rel. change to Start variant
Start		4.385	
V11	Volume / Efficiency	3.866	-11.8%
V14	Volume	2.906	-33.7%
V31	Efficiency (29.1%)	4.427	0.9%
V52	Efficiency (38.7%)	3.799	-13.4%

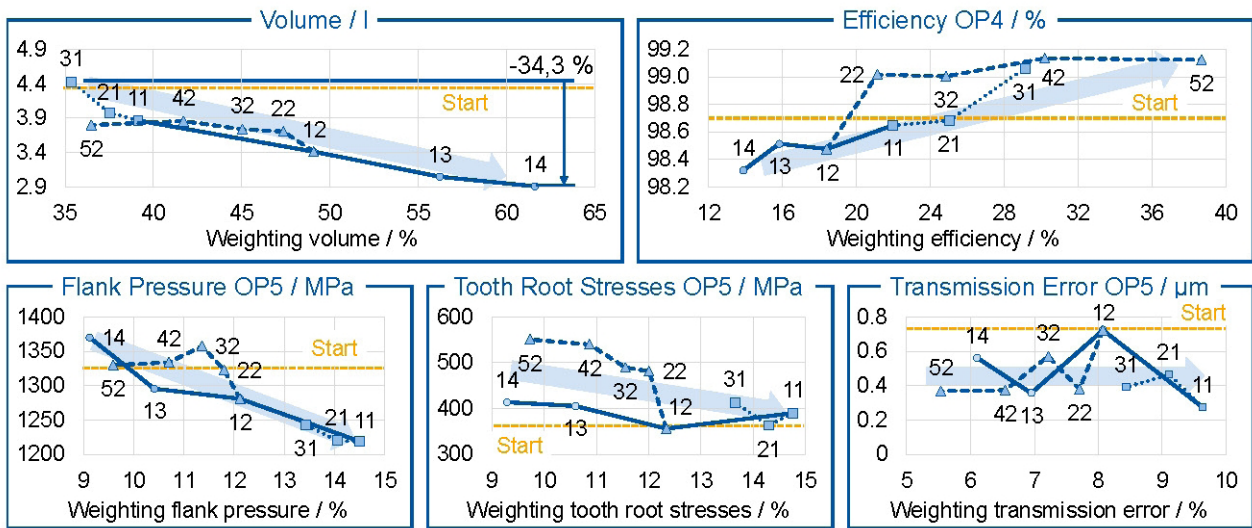


Figure 10 Comparison of the Resulting Key Values of the Different Optimization Variants

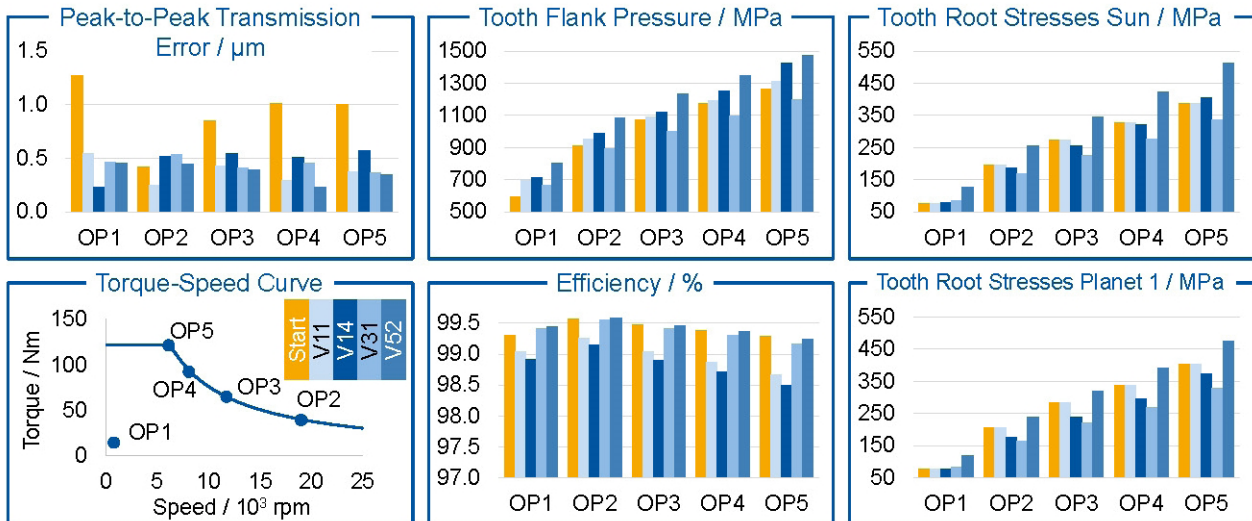


Figure 11 Results of the Selected Variants (Sun – Planet 1 Mesh)

The calculation results of the four selected variants are shown for the sun-planet 1 mesh in Figure 11. First, the significantly lower peak-to-peak transmission error of all optimized variants can be seen. The results for the load-carrying capacity (tooth flank pressure and tooth root stress) of the balanced weighting variant V11 are comparable to those of the variant Start. The volume-optimized variant V14 and the efficiency-optimized variant V52 show a higher tooth flank pressure. On the one hand, this is due to a smaller center distance of both variants and, on the other hand, to a smaller normal module of variant V52. Due to the smaller normal module of variant V52, the tooth root stress of this variant is the highest. The efficiency of variant V31 and variant V52 is comparable to that of variant Start. The assumption that the higher volume of variant V31 compared to variant V52 has a positive influence on the load-carrying capacity with comparable efficiency is shown.

The results for the planet 2-ring gear mesh are shown in Figure 12. The peak-to-peak transmission error is comparable for all variants. The variant Start has the lowest tooth root stress and at the same time the highest tooth flank pressure. The optimized variants offer a more balanced design in terms of load-carrying capacity. The efficiency of the variant Start is the lowest together with the volume-optimized variant V14. The tooth root stress of variant V52 shows the highest value for both gears. The efficiency of variants V31 and V52 is similar and comparatively higher than that of the other variants.

In summary, variant V14, with slightly lower efficiency in the sun-planet 1 mesh, enables a 33.7% reduction in volume. With variant V11, a reduction in excitation is possible with comparable overall efficiency and a simultaneous reduction in volume of 11.8%. The variants V31 and V52 offer increased efficiency and lowered excitation. Depending on the additional dynamic loads and the other boundary conditions of the application, it must be weighted higher for variants V31 and V52 whether the lower volume of variant V52 or the higher load-carrying capacity of variant V31 is more appropriate.

Summary and Outlook

In applications with a high power density and high gear ratio requirements, such as electrically driven vehicles, stepped planetary gear stages can be used. The design of planetary and stepped planetary gear stages is related to assembly restrictions due to their kinematic overdetermination. Generally, numerical optimization methods are increasingly used for gear design. Due to the high number of different design variables for stepped planetary gear stages, optimization methods are suitable for the design and optimization.

The objective of this paper is to develop a method for the algorithm-based design and optimization of the macrogeometry of stepped planetary gear stages. For this purpose, a method for the identification of suitable tooth number combinations is presented first. The developed optimization method offers the advantage of an FE-based evaluation of the operational behavior. A particle swarm algorithm is used to optimize 18 geometry parameters. In the optimization, different operating conditions are considered and weighted against each other.

The developed method is applied to the design and optimization of a stepped planetary gear stage for an electrically driven compact car. For this purpose, ten differently weighted variants are defined and compared. The volume, the efficiency, the peak-to-peak transmission error, the tooth flank pressure, and the tooth root stresses are used as evaluation variables. The weighting components' *efficiency* and *volume* are varied for the different variants.

A comparison of the objective values of the different optimization variants shows a very good correlation between the weighting of an optimization objective and its value. The volume of the gear stage can be reduced by 33.7% for the volume-optimized variant V14. Despite this increase in power density, the characteristic values of the load-carrying capacity of this variant are comparable to those of the initial variant, and the efficiency is only slightly lower. The two other weighting variants analyzed in detail, V31 and V52, offer higher average efficiency than the initial variant.

Overall, the developed method shows further potential in the design and optimization of stepped planetary gear stages. The

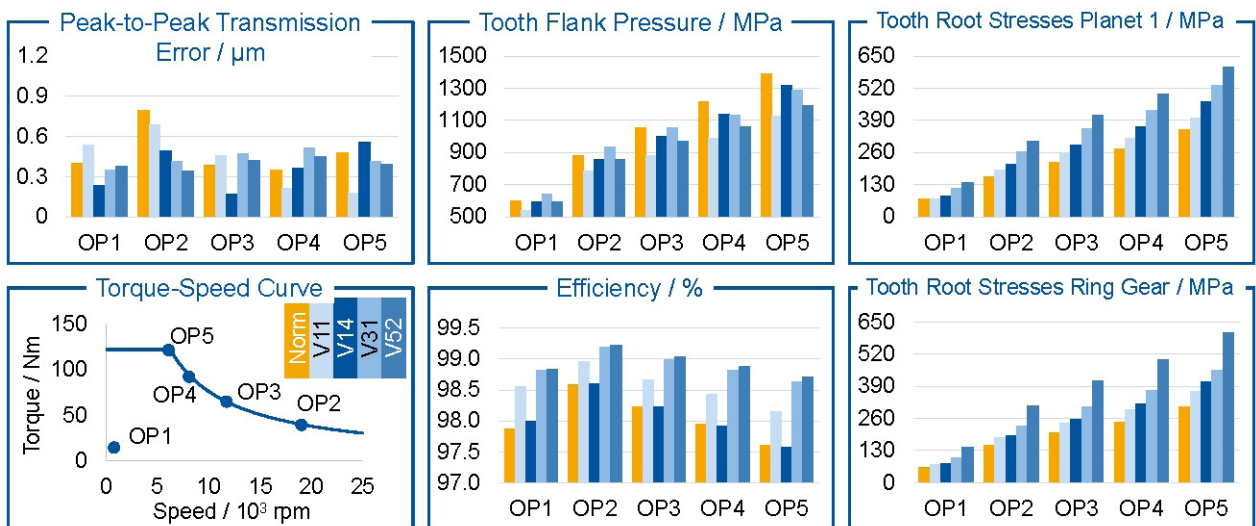


Figure 12 Results of the Selected Variants (Planet 2 – Ring Gear Mesh)

operational behavior of the different optimization variants can be evaluated for a final selection in the multi-body simulation under dynamic operating conditions. Furthermore, an optimization of the microgeometry should be performed, considering the interaction and displacements of the gears. ⚙️

Bibliography

1. Klocke F; Brecher C., 2017: Zahnrad- und Getriebetechnik. 1. Aufl, München: Carl Hanser.
2. Norm, 2006: Calculation of load capacity of spur and helical gears. Calculation of surface durability (pitting) (6336 Part 2): Beuth, Berlin.
3. Cao J., 2002: Anforderungs- und fertigungsgerechte Auslegung von Stirnradverzahnungen durch Zahnkontaktanalyse mit Hilfe der FEM. Diss. RWTH Aachen University.
4. Hemmelmann J. E., 2007: Simulation des lastfreien und belasteten Zahneingriffs zur Analyse der Drehübertragung von Zahnradgetrieben. Diss. RWTH Aachen University.
5. Kohn B., 2019: Topologische Flankenkorrektur zur Anregungsoptimierung von Stirnradgetrieben. Diss. TU München.
6. Brimmers J., 2020: Funktionsorientierte Auslegung topologischer Zahnflankenmodifikationen für Beveloidverzahnungen. Diss. RWTH Aachen University.
7. Müller H. W., 1998: Die Umlaufgetriebe. 2. Aufl, Berlin: Springer.

Christian Westphal has been the leader of the Gearbox NVH group at the Laboratory for Machine Tools and Production Engineering (WZL) of RWTH Aachen University since April 2022. His research focuses on the design and the dynamic operational behavior of planetary gearboxes. Westphal graduated from RWTH Aachen University with a master's degree in industrial engineering and management with a major in automotive engineering and corporate development.



Dr.-Ing. Jens Brimmers is the head of the gear department at the Laboratory for Machine Tools and Production Engineering (WZL) of RWTH Aachen University since June 2019. He graduated from RWTH Aachen University with master's degrees in mechanical engineering and business administration. His Ph.D. thesis focused on beveloid gears and topological tooth flank modification.



Prof. Dr.-Ing. Christian Brecher has since January 2004 been Ordinary Professor for Machine Tools at the Laboratory for Machine Tools and Production Engineering (WZL) of the RWTH Aachen, as well as Director of the Department for Production Machines at the Fraunhofer Institute for Production Technology IPT. Upon finishing his academic studies in mechanical engineering, Brecher started his professional career first as a research assistant and later as team leader in the department for machine investigation and evaluation at the WZL. From 1999 to April 2001, he was responsible for the department of machine tools in his capacity as a Senior Engineer. After a short spell as a consultant in the aviation industry, Professor Brecher was appointed in August 2001 as the Director for Development at the DS Technologie Werkzeugmaschinenbau GmbH, Mönchengladbach, where he was responsible for construction and development until December 2003. Brecher has received numerous honors and awards, including the Springorum Commemorative Coin; the Borchers Medal of the RWTH Aachen; the Scholarship Award of the Association of German Tool Manufacturers (Verein Deutscher Werkzeugmaschinenfabriken VDW); and the Otto Kienzler Memorial Coin of the Scientific Society for Production Technology (Wissenschaftliche Gesellschaft für Produktionstechnik WGP).

